AIAA JOURNAL
Vol. 39, No. 1, January 2001

Similarity Analysis for Turbulent Boundary Layer with Pressure Gradient: Outer Flow

Luciano Castillo*
Rensselaer Polytechnic Institute, Troy, New York 12180
and
William K. George†
State University of New York at Buffalo, Buffalo, New York 14260

The equilibrium-type similarity analysis of George and Castillo for the outer part of zero pressure gradient boundary layers (George, W. K., and Castillo, L., "Zero Pressure Gradient Turbulent Boundary Layer," *Applied Mechanics Reviews*, Pt. 1, Vol. 50, No. 11, 1997, pp. 689–729) has been extended to include boundary layers with pressure gradient. The constancy of a single new pressure gradient parameter is all that is necessary to characterize these new equilibrium turbulent boundary layers. Three major results are obtained: First, most pressure gradient boundary experiments appear to be equilibrium flows (by the new definition), and nonequilibrium flows appear to be the exception. Second, there appear to be only three values of the pressure gradient parameter: one for adverse pressure gradients, one for favorable pressure gradients, and one for zero pressure gradients. Third, correspondingly, there appear to be only three normalized velocity deficit profiles, exactly as suggested by the theory.

Nomenclature

f_{op}	=	outer velocity profile (at finite δ^+)
$f_{\mathrm{op}\infty}$	=	asymptotic outer velocity profile (as $\delta^+ \to \infty$)
R_{so}	=	outer Reynolds stress scale
Re_θ	=	Reynolds number based on θ
U_{so}	=	outer velocity scale
U_∞	=	freestream velocity
$U_\infty - U$	=	velocity deficit
$U_{\infty i}$	=	freestream velocity at first measured position
$U_\infty(\delta_*/\delta)$	=	Zagarola/Smits velocity scale
u_*	=	friction velocity, $\sqrt{(\tau_w/\rho)}$
$\bar{y}$	=	y/δ
β	=	Clauser pressure parameter, $(\delta_*/\rho u_*^2)\,\mathrm{d}P_\infty/\mathrm{d}x$
δ	=	boundary-layer thickness, for example, δ_{99}
δ_*	=	displacement thickness, $\int_0^\infty \left(1 - \frac{U}{U_\infty}\right)\mathrm{d}y$
δ^+	=	$\delta u_*/\nu$
θ	=	momentum thickness $\int_0^\infty \left(\frac{U}{U_\infty}\right)\left(1 - \frac{U}{U_\infty}\right)\mathrm{d}y$
θ_i	=	momentum thickness at first measured position
Λ	=	pressure parameter, identical to $\frac{\delta}{\rho U_\infty^2\,\mathrm{d}\delta/\mathrm{d}x}\frac{\mathrm{d}P_\infty}{\mathrm{d}x}$
$*$	=	(unknown) dependence on upstream conditions

Introduction

THIS paper will show that it is possible to find similarity solutions of the equations governing the outer part of a two-dimensional (in the mean), stationary, incompressible boundary layer on a smooth surface with externally imposed pressure gradient. Moreover, it will be shown that these solutions are in remarkable agreement with the abundant experimental data that have been accumulated on such boundary layers over the past 50 years. Surprisingly, it will be seen that the velocity profiles of all such pressure gradient boundary layers can be reduced to only three profiles: one each for zero pressure gradient (ZPG), adverse pressure gradient (APG), and favorable pressure gradient (FPG) boundary layers. These will be shown to correspond to three distinct values of the pressure gradient similarity parameter Λ, which appear to characterize all flows.

The results presented extend the ZPG analysis of George and Castillo[1] to include pressure gradients and supersede the earlier paper on this subject.[2] The similarity solutions obtained can, in fact, be identified as the equilibrium solutions originally sought by Clauser,[3,4] who unfortunately overconstrained the problem by imposing a single velocity scale u_*. This overconstraint led Clauser to a definition of equilibrium boundary layers [$\beta = (\delta_*/\rho u_*^2)\,\mathrm{d}P_\infty/\mathrm{d}x = \text{const}$] that was not satisfied by most experimental flows. In fact, it is commonly believed that equilibrium boundary layers are nearly impossible to generate and maintain, and the few cases where they have been approximated were obtained with great difficulty by adjusting the pressure gradient along the flow (see Refs. 3–6).

The definition of equilibrium boundary layers derived herein, that is, $\Lambda \equiv \delta/(\mathrm{d}\delta/\mathrm{d}x)(1/\rho U_\infty^2)\,\mathrm{d}P_\infty/\mathrm{d}x = \text{const}$, will be seen to be satisfied by nearly all boundary layers. Moreover, even when the external conditions are changed, for example, from positive to negative pressure gradient, it appears that the boundary layer rapidly settles into a new equilibrium if it does not separate or relaminarize.

Similarity Analysis

The equations and boundary conditions governing at least the outer 90% of a turbulent boundary layer at high Reynolds number with pressure gradient are given by Townsend[7,8] as follows.

The x momentum:

$$U\frac{\partial U}{\partial x} + V\frac{\partial U}{\partial y} = -\frac{1}{\rho}\frac{\mathrm{d}P_\infty}{\mathrm{d}x} + \frac{\partial}{\partial y}[-\langle uv\rangle] + \frac{\partial}{\partial x}[\langle v^2\rangle - \langle u^2\rangle] \quad (1)$$

The continuity:

$$\frac{\partial U}{\partial x} + \frac{\partial V}{\partial y} = 0 \quad (2)$$

Received 17 November 1999; presented as Paper 2000-0193 at the 38th Aerospace Sciences Meeting, Reno, NV, 11–14 January 2000; revision received 22 May 2000; accepted for publication 24 May 2000.

*Assistant Professor, Department of Mechanical Engineering, Aeronautical Engineering and Mechanics.
†Professor, Department of Mechanical and Aerospace Engineering.

where $U \to U_\infty$ and $-\langle uv \rangle \to 0$ as $y \to \infty$. Note that the viscous terms in the momentum equation have been neglected because they are small away from the near-wall region, that is, when $y > 100\nu/u_*$ or $y^+ > 100$ typically. Also, the last terms on the right-hand side are of second order in the turbulence intensity and are usually neglected.

These equations are approximately valid for large finite values of the local Reynolds number; that is, $\delta^+ = \delta u_*/\nu > 500$, where δ^+ is the ratio of inner to outer length scales.[1] Most important, Eq. (1) becomes exact in the limit as $\delta^+ \to \infty$. Because in this limit the outer boundary layer equations are independent of Reynolds number, the properly scaled velocity and Reynolds stress profiles for the outer region must also be independent of Reynolds number. This is the asymptotic invariance principle (AIP) described by George[9] and used by George and Castillo[1] for the ZPG boundary-layer and George et al.[10] for pipe and channel flows. In other words, the AIP simply means that in the limit as the Reynolds number dependence goes to infinity the equations of motions become independent of Reynolds number; thus, any function or scale must also be independent of Reynolds number, however, only in this limit.

In accordance with the AIP, solutions will be sought that reduce to similarity solutions of the outer momentum equation and boundary conditions in the limit of infinite local Reynolds number. This limit can be achieved by increasing the distance along the plate from the leading edge for fixed upstream conditions. That is, the conditions at leading edge of test surface are kept constant, for example, the wind-tunnel speed, size of tripping wire, surface conditions, constant suction velocity, or any other possible external condition that may affect the downstream flow.

Remember that unlike the analyses of Clauser[3,4] or Townsend[8] (see also Ref. 11), no scaling laws will be assumed at the outset. Rather, the outer scale quantities (such as U_{so} and R_{so}) will be derived from the conditions for similarity of the equations, thus ensuring that the scaled profiles are invariant in the limit of infinite local Reynolds number.

Similarity solutions for the mean velocity and Reynolds shear stress profiles will be sought of the following forms:

$$U - U_\infty = U_{so}(x) f_{op}(\bar{y}, \delta^+, \Lambda, *) \tag{3}$$

$$-\langle uv \rangle = R_{so}(x) r_{op}(\bar{y}, \delta^+, \Lambda; *) \tag{4}$$

where the pressure gradient parameter Λ accounts for the freestream pressure gradient and will be defined later using the equations of motion. Also, the argument $*$ represents a possible (and what will be seen to be actual) dependence of the flow on upstream conditions, the causes of which are to this point unknown. U_{so} and R_{so} are to be determined only from the equations of motion and represent the outer mean velocity and Reynolds shear stress scales, respectively. The similarity variable is $\bar{y} = y/\delta$, where δ is the boundary-layer thickness, for example, δ_{99} or δ_{95}. The local Reynolds number dependence of the profiles is represented by the presence of the argument δ^+.

The velocity in Eq. (3) has been written in deficit form to avoid the necessity of accounting for its variation across the inner layer, the very near-wall region (which is not of direct interest in this paper). This is not necessary with the Reynolds stress because it vanishes outside the boundary layer. Note again that the outer velocity scale U_{so} and the Reynolds shear stress R_{so} must both be determined from the boundary-layer equations only and cannot be chosen a priori nor imposed from ad hoc arguments.

Because in the infinite local Reynolds number limit, the outer equations become independent of δ^+, so must the solutions to them. Hence, in this limit, Eqs. (3) and (4) must also become independent of Reynolds number (as required by the AIP), that is,

$$f_{op}(\bar{y}, \delta^+, \Lambda; *) \to f_{op\infty}(\bar{y}, \Lambda; *) \tag{5}$$

$$r_{op}(\bar{y}, \delta^+, \Lambda; *) \to r_{op\infty}(\bar{y}, \Lambda; *) \tag{6}$$

as $\delta^+ \to \infty$. The subscript op∞ is used to distinguish these infinite Reynolds number solutions from the finite Reynolds number profiles used before [Eqs. (3) and (4)]. There is nothing in the equations themselves to suggest that the dependence on upstream conditions $*$ can be removed, and so it has to be retained.

Substituting Eqs. (5) and (6) into Eq. (1) and clearing terms yield

$$\begin{pmatrix} \delta & \mathrm{d}U_\infty \\ U_{so} & \mathrm{d}x \end{pmatrix} + \begin{pmatrix} U_\infty \\ U_{so} \end{pmatrix} \begin{matrix} \delta & \mathrm{d}U_{so} \\ U_{so} & \mathrm{d}x \end{matrix} \Bigg) f_{op\infty}$$

$$+ \begin{pmatrix} \delta & \mathrm{d}U_{so} \\ U_{so} & \mathrm{d}x \end{pmatrix} f_{op\infty}^2 - \begin{pmatrix} U_\infty & \mathrm{d}\delta \\ U_{so} & \mathrm{d}x \end{pmatrix} + \begin{matrix} \delta & \mathrm{d}U_\infty \\ U_{so} & \mathrm{d}x \end{matrix} \Bigg) \bar{y} f'_{op\infty}$$

$$- \begin{pmatrix} \mathrm{d}\delta \\ \mathrm{d}x \end{pmatrix} + \begin{matrix} \delta & \mathrm{d}U_{so} \\ U_{so} & \mathrm{d}x \end{matrix} \Bigg) f'_{op\infty} \int_0^{\bar{y}} f_{op\infty}(\tilde{y})\, \mathrm{d}\tilde{y} = \begin{pmatrix} Re_{so} \\ U_{so}^2 \end{pmatrix} r'_{op\infty} \tag{7}$$

where the term involving $-\mathrm{d}P_\infty/\mathrm{d}x$ has been canceled by the $\rho U_\infty\, \mathrm{d}U_\infty/\mathrm{d}x$ term from Euler's equation for the external flow.

For the particular type of equilibrium similarity solutions suggested by George[9,12] (and applied by George and Castillo[1] to the ZPG boundary layer), all of the terms in the governing equations must maintain the same relative balance as the flow develops. These equilibrium similarity solutions exist only if all of the square bracketed terms have the same x dependence and are independent of the similarity coordinate $\bar{y}$. Thus the bracketed terms must remain proportional to each other as the flow develops, that is,

$$\begin{matrix} \delta & \mathrm{d}U_{so} \\ U_{so} & \mathrm{d}x \end{matrix} \sim \begin{matrix} \delta & \mathrm{d}U_\infty \\ U_{so} & \mathrm{d}x \end{matrix} \sim \begin{pmatrix} U_\infty \\ U_{so} \end{pmatrix} \begin{matrix} \delta & \mathrm{d}U_{so} \\ U_{so} & \mathrm{d}x \end{matrix} \sim \begin{matrix} \mathrm{d}\delta \\ \mathrm{d}x \end{matrix}$$

$$\sim \begin{pmatrix} U_\infty \\ U_{so} \end{pmatrix} \begin{matrix} \mathrm{d}\delta \\ \mathrm{d}x \end{matrix} \sim \begin{matrix} Re_{so} \\ U_{so}^2 \end{matrix} \tag{8}$$

where $\sim$ means has the same x dependence as.

It is clear that (just as for the ZPG boundary layer), full similarity (of the equilibrium-type) is possible only if

$$U_{so} \sim U_\infty \tag{9}$$

$$R_{so} \sim U_{so}^2 \frac{\mathrm{d}\delta}{\mathrm{d}x} \sim U_\infty^2 \frac{\mathrm{d}\delta}{\mathrm{d}x} \tag{10}$$

Thus, the outer equations do admit to full similarity solutions in the limit of infinite Reynolds number, and these solutions determine the outer scales. No other choice of scales can produce profiles (of the assumed form) that are asymptotically independent of the local Reynolds number, at least unless they reduce to these scales in the limit.

There are several additional independent constraints given by

$$\begin{matrix} \mathrm{d}\delta \\ \mathrm{d}x \end{matrix} \sim \begin{matrix} \delta & \mathrm{d}U_\infty \\ U_\infty & \mathrm{d}x \end{matrix} \sim \begin{matrix} \delta & \mathrm{d}P_\infty \\ \rho U_\infty^2 & \mathrm{d}x \end{matrix} \tag{11}$$

Note that the pressure gradient controls the growth rate of the boundary layer. A surprising consequence of this condition is that it is satisfied by a power law relation between the freestream velocity and the boundary-layer thickness, that is,

$$\delta \sim U_\infty^n \tag{12}$$

where n can, to this point at least, be any nonzero constant. This is the reminiscent of familiar Falker–Skan (FS) solutions of laminar boundary layers with pressure gradient (cf. Batchelor[13]), but with δ as the variable instead of x. (Not surprisingly, the AIP methodology applied to the laminar flow equations leads to more general forms of the FS solutions as well, but this is a paper about turbulence.) Note that Eq. (12) indeed implies that if U_∞ can be represented as a power of x, then δ must also be a power of x. There is, of course, no reason at all to consider only flows in which U_∞ is a power of x because the result of Eq. (12) is much more general. In fact, it will be seen later to apply to nearly all experimental flows.

The pressure gradient parameter Λ can be defined as

$$\Lambda \equiv \begin{matrix} \delta & \mathrm{d}P_\infty \\ \rho U_\infty^2\, \mathrm{d}\delta/\mathrm{d}x & \mathrm{d}x \end{matrix} = \text{const} \tag{13}$$

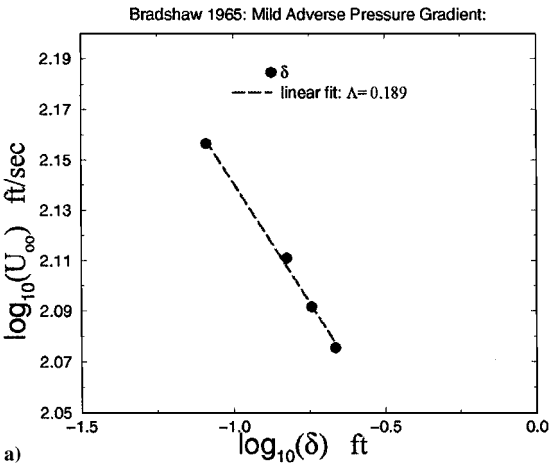

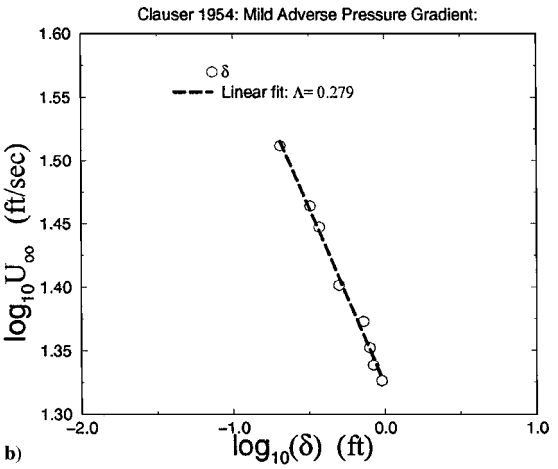

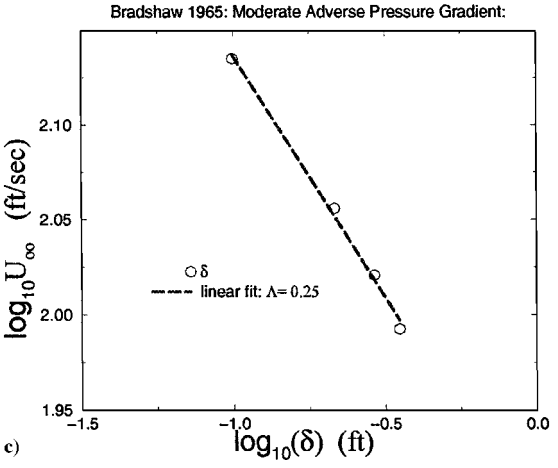

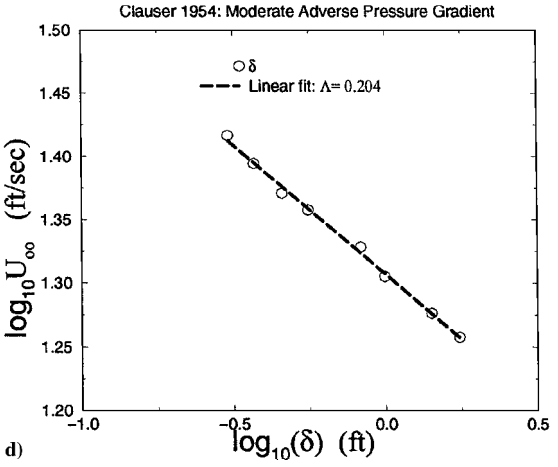

Fig. 1 Log–log plots of U_∞ vs δ_{99} along with fit of $\delta_{99} \sim U_\infty^{-1/\Lambda}$ using stated value of Λ.

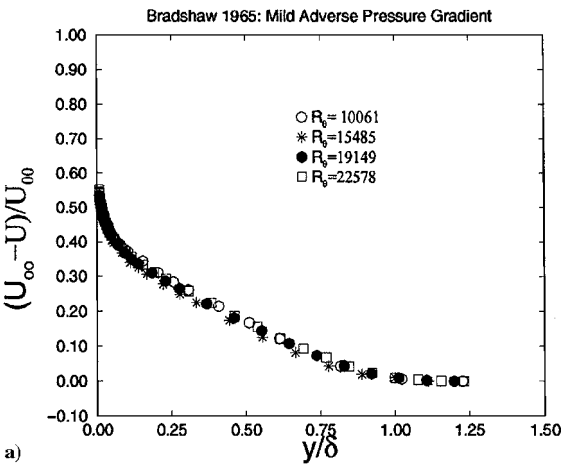

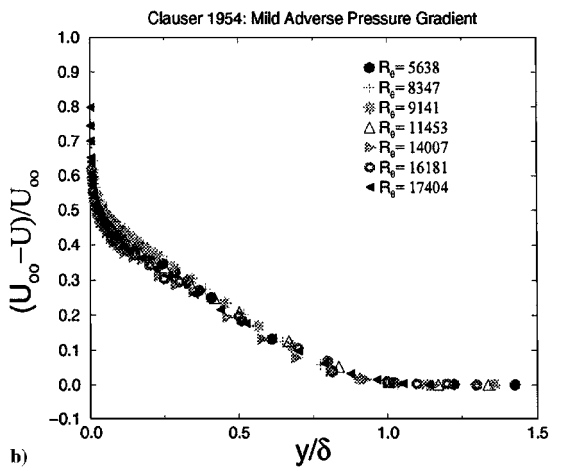

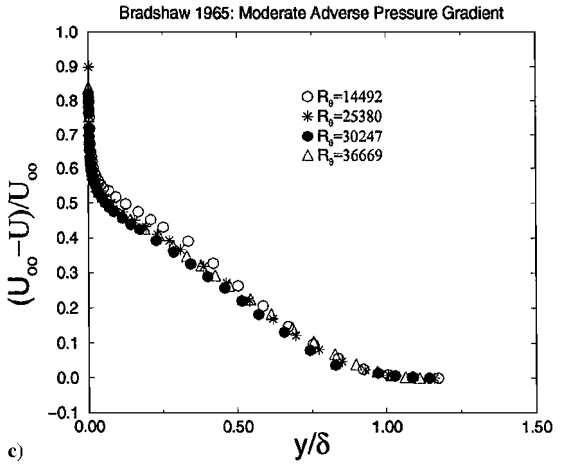

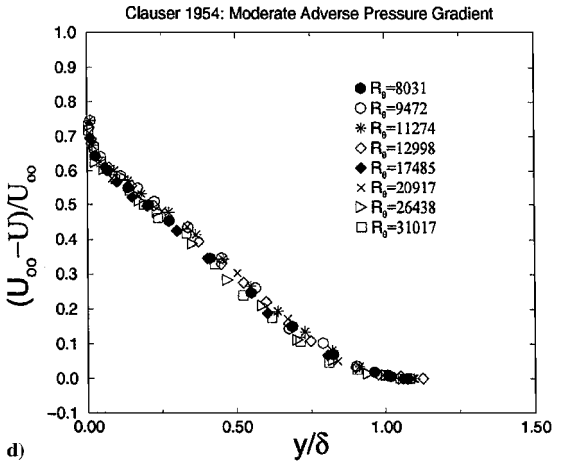

Fig. 2 Velocity profiles in adverse pressure gradient normalized with U_∞ and δ_{99}.

or equivalently

$$\Lambda \equiv -\frac{\delta}{U_\infty\, \mathrm{d}\delta/\mathrm{d}x}\frac{\mathrm{d}U_\infty}{\mathrm{d}x} = \text{const} \tag{14}$$

Because equilibrium flows require $\Lambda = \text{const}$ for similarity, Eq. (14) can be integrated (for nonzero values of Λ) to obtain

$$\delta \sim U_\infty^{-1/\Lambda} \tag{15}$$

Thus, not only there is a power law relation between the boundary-layer thickness and the imposed freestream velocity, but the exponent is determined uniquely by the pressure gradient parameter, that is,

$$n = -1/\Lambda \tag{16}$$

Therefore, an equilibrium boundary layer in the present approach is one where $\Lambda = \text{const}$ and (when $\Lambda \neq 0$), $\delta \sim U_\infty^{-1/\Lambda}$. Because it is the freestream velocity, U_∞ (or $\mathrm{d}P_\infty/\mathrm{d}x$), which is usually imposed on the boundary layer by external means, this is a remarkably restrictive constraint on δ. As a consequence it provides a powerful experimental test of the present theory; surprisingly, most experiments will be seen to satisfy this equilibrium condition.

Results

Over the past six decades a great deal of data on simple boundary layers have been accumulated. The goal here is to examine whether the similarity theory just developed is consistent with these data. There are two primary criteria for this evaluation.

First, the similarity condition unique to pressure gradient boundary layers, namely, $\delta \sim U_\infty^{-1/\Lambda}$, with $\Lambda = \text{const}$ will be checked using the abundant experimental data, primarily from Coles and Hirst.[14] For this, the reported values of δ_{99} will be used along with the reported values of U_∞. The latter will be used interchangeably with U_{edge} (when provided by the authors) because these seldom differ by more than a few percent. When δ_{99} has not been given in the data set, it has been calculated from the profiles. Note that δ_{95} or δ_{90} could have as easily been used, and perhaps with less error in their determination. Also, the plots will be given in dimensional form using the original dimensions reported by the investigators to avoid any confusion as to precisely which data were used.

Second, the whole question of whether U_∞ is an appropriate scale for the outer velocity profile will be checked. This will be accomplished by plotting $(U_\infty - U)/U_\infty$ vs $\bar{y} = y/\delta$. The cited values for the velocity data will be used together with the values of U_∞ and δ_{99} determined earlier.

Note that the theory does not imply that U_∞ must necessarily collapse the data into a single curve. It only implies that the profiles normalized by U_∞ should be converging toward an asymptote as the local Reynolds number increases. Note also that the profiles from different upstream conditions do not necessarily have to collapse to the same asymptotic profile because an asymptotic dependence on these upstream conditions cannot be ruled out.

APG: $\Lambda > 0$

Figures 1a–1d and 2a–2d display the data for four different experimental adverse pressure gradient boundary layers: the mild and moderate APG experiments from Clauser[3] and Bradshaw.[5]

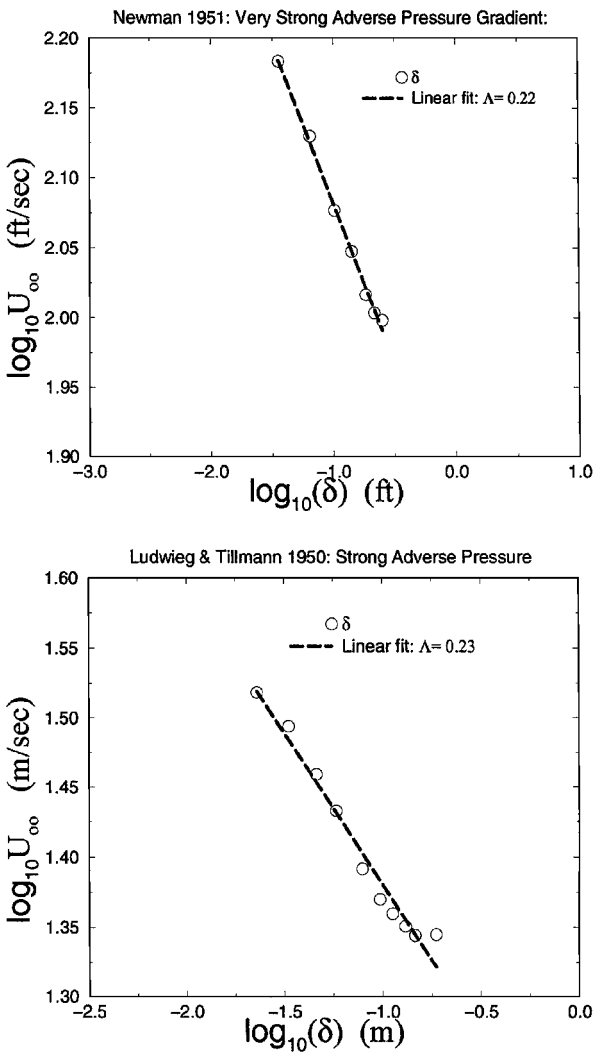

Fig. 3 Strong APG boundary layers very near to separation and with eventual separation; log–log plots of U_∞ vs δ_{99} along with fit of $\delta_{99} \sim U_\infty^{-1/\Lambda}$ using stated value of Λ.

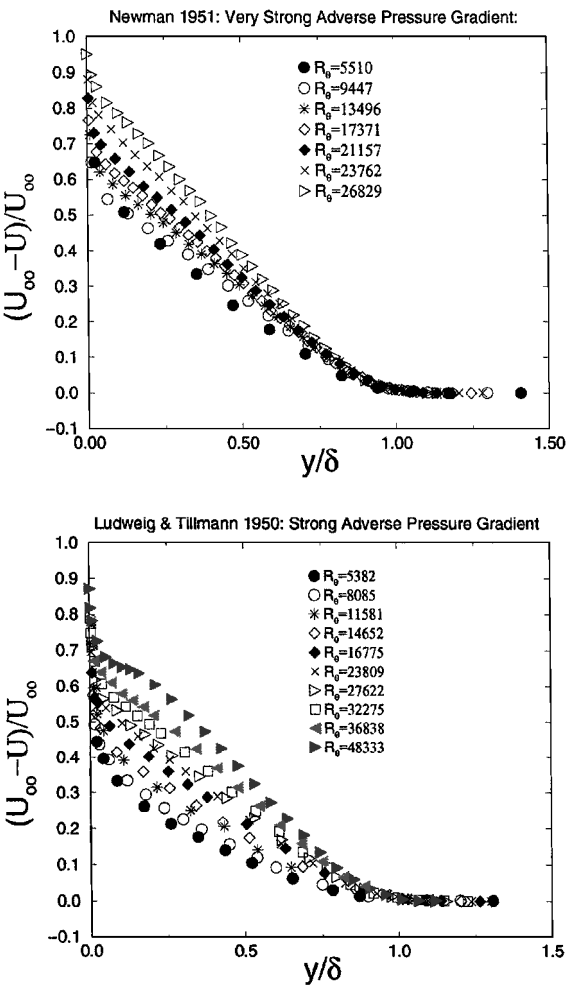

Fig. 4 Strong APG boundary layers very near to and with eventual separation; velocity profiles for same data normalized by U_∞ and δ_{99}.

Figures 1a–1d show log–log plots in dimensional variables of U_∞ vs δ_{99} (similarity condition), along with a power law fit to each data set. These curves are linear on a log–log plot, and their slope is $-\Lambda$, the similarity parameter of primary interest. Obviously the data are all in excellent agreement with the equilibrium similarity requirement. This is particularly convincing with the data sets that have the most points. The individual values of Λ determined from fitting the entire data set are quite close, ranging from 0.189 to 0.279. As will be shown later, they could have been taken as equal with little change in the fit. This is quite a surprising result, given the range of pressure gradients involved.

Figures 2a–2d show the corresponding velocity profiles plotted as a deficit and normalized by U_∞ and δ_{99}. The collapse of the profiles is striking, especially in view of the range of Reynolds numbers within each data set. In fact, the collapse of the profiles for each experiment is so good it is surprising that it has not been noticed before. Note, for later reference that the upstream conditions were fixed for each data set (by the investigators), and all of the variation in Reynolds number is due to the downstream development of the flow.

Figures 3 and 4 show two more data sets for adverse pressure gradient boundary layers very close to separation (and they in fact eventually do separate[6,15]). The plots of U_∞ vs δ_{99} of Fig. 3 fall nearly on the same power law curve with $\Lambda = 0.22$ and 0.23, respectively. It is easy to see where the boundary is about to separate (or has done so already) by the departure from the power law curve of the last point or two from the bottom. The velocity profile plots normalized by U_∞ and δ_{99} of Fig. 4 do not collapse like those show earlier, although the spread is reduced if the last few profiles are removed. On the other hand, (as will be shown) they can be collapsed using the factor of δ_*/δ suggested by Zagarola and Smits.[16] Regardless, the similarity theory does not imply that U_∞ is a velocity scale that should collapse the data at finite Reynolds number, its success with the experiments earlier notwithstanding. The AIP implies only that the profiles scaled in this manner should be asymptotically independent of Reynolds number. There is certainly some suggestion from Figs. 3 and 4 that this might be the case, at least if the curves closest to separation are not considered.

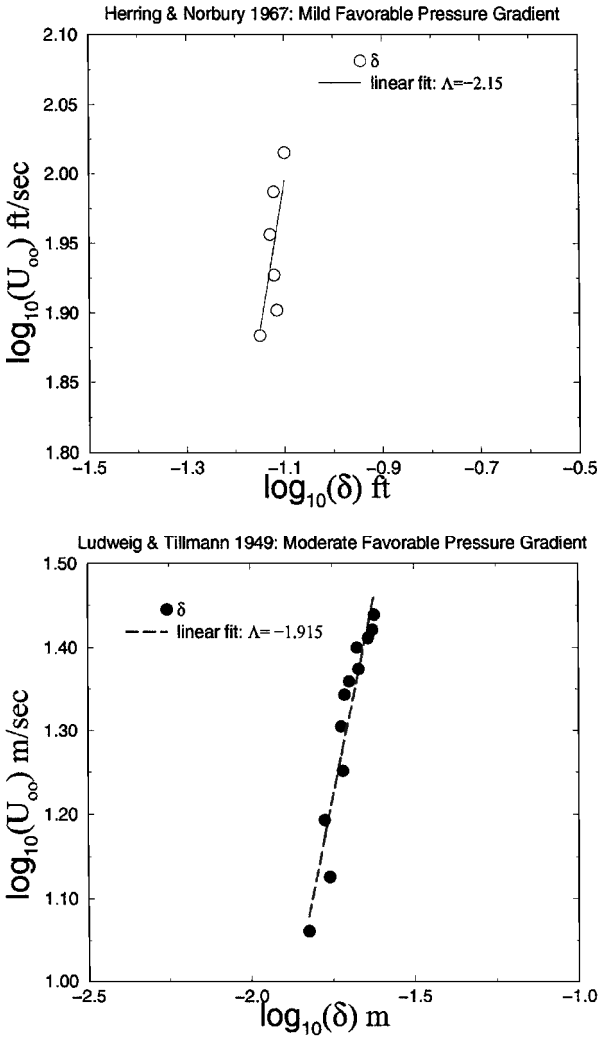

Fig. 5 Representative FPG boundary layers; log–log plots of U_∞ vs δ_{99} along with fit of $\delta_{99} \sim U_\infty^{-1/\Lambda}$ using stated value of Λ.

FPG: $\Lambda < 0$

Figures 5 and 6 show the data for two different experimental FPG boundary layers: the mild FPG experiment of Herring and Norbury[17] and the moderate FPG experiment of Ludwieg and Tillmann.[6] Figure 5 shows log–log plots in dimensional variables of U_∞ vs δ_{99}, along with a power law fit to each data set. Again, the data are all in excellent agreement with the equilibrium similarity requirement. The slopes of the fitted curves are $-\Lambda = 2.15$ and 1.92, respectively. Also, the mean velocity profiles normalized with U_∞ and δ_{99} nearly collapse as shown in Fig. 6.

Three Profiles

As noted, it appears that all APG boundary layers might be characterized by a single value of Λ ($\Lambda \approx 0.22$). Also all FPG boundary layers appear to be characterized by a single value of Λ ($\Lambda \approx -1.92$). Figure 7a shows all of the APG data of Figs. 1 and 3 plotted together, and Fig. 7b shows all of the FPG plots of Fig. 5 and from Kline et al.[18] plotted together. Figure 7 confirms that only two values of Λ are necessary for all boundary layers with pressure gradient: 0.22 (APG) and -1.92 (FPG). A third value of $\Lambda = 0$ can be included to cover the ZPG case. Note that the freestream velocity U_∞ has been arbitrarily normalized by the freestream velocity at the first measured position $U_{\infty i}$. Similarly, the boundary-layer thickness has been normalized by the momentum thickness θ_i at the same location.

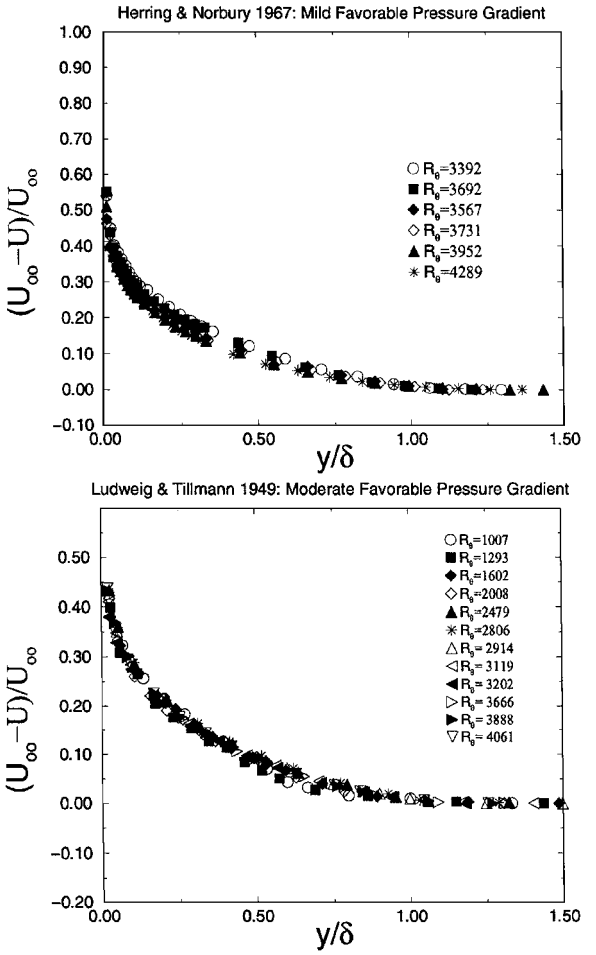

Fig. 6 Representative FPG boundary layers; velocity profile normalized with U_∞ and δ_{99}.

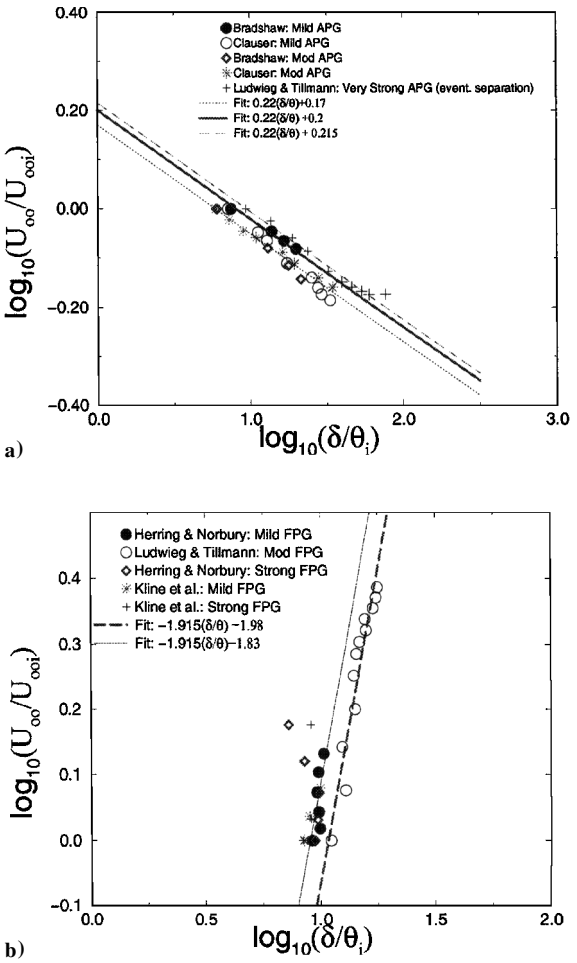

Fig. 7 U_∞ vs δ_{99} (normalized with $U_{\infty i}$ and θ_i for first measured location) for all data of a) APG and b) FPG.

These results appear to hold for all boundary layers considered, whether previously believed to be in equilibrium or not, and are independent of the strength (weak, mild, strong) of the pressure gradient. The only exceptions were experiments undergoing rapid changes, but even these appeared to settle quickly into one of these three equilibrium states. Most interesting was the experiment of Schubauer and Klebanoff[19] (not shown), which began with an FPG, then evolved to a near-ZPG, and finally an APG with eventual separation. The first three phases of this experiment were consistent with the equilibrium similarity states identified earlier and evolved rapidly from one equilibrium similarity state to another when the imposed pressure gradient was changed.

In similarity variables, the outer mean momentum equation in the limit of infinite Reynolds number Eq. (7) reduces to

$$-\Lambda\left(2f_{\mathrm{op}\infty} + f_{\mathrm{op}\infty}^2\right) + (\Lambda - 1)\bar{y}f'_{\mathrm{op}\infty} + (\Lambda - 1)f'_{\mathrm{op}\infty}\int_0^{\bar{y}} f_{\mathrm{op}\infty}\,\mathrm{d}\rho = \bar{r}'_{\mathrm{op}\infty} \tag{17}$$

where the factor of $R_{\mathrm{so}}/[U_{\mathrm{so}}^2\,\mathrm{d}\delta/\mathrm{d}x]$ has been absorbed (without loss of generality) into r'_{op}. If there are only three possible values of Λ (0, 0.22, −1.92), then there can only be three asymptotic solutions: one each for ZPG, APG, and FPG. In particular, this implies that all velocity deficit profiles for all boundary layers (at least equilibrium by our definition) should reduce to only three curves.

In Fig. 8a, all of the adverse velocity (APG) profiles of Figs. 2 and 4 are plotted together, but now normalized using $U_\infty\,\delta_*/\delta_{99}$ and δ_{99}. It is clear from the velocity profile plots of Figs. 2 and 6 that U_∞ alone was enough to collapse most of the data for fixed upstream conditions. Here, however, profiles are being plotted together for a variety of upstream conditions, and they do not collapse together with U_∞ alone. Castillo[20] has recently shown, however, that the scale velocity $U_\infty\,\delta_*/\delta_{99}$ (originally suggested by Zagarola and Smits[16]) effectively removes the effects of both the upstream conditions and finite local Reynolds number on the outer velocity profile of ZPG and pressure gradient boundary layers. Because the ratio of δ_*/δ is constant in the limit of infinite Reynolds number (see George and Castillo[1] and Castillo[20]), it follows that the profiles normalized in this manner represent the asymptotic profile $f_{\mathrm{op}\infty}(\bar{y}, \Lambda)$. Figure 8b shows the FPG profiles normalized in a similar manner; again the profiles collapse. A theoretical justification of the Zagarola and Smits scaling for boundary layers with ZPG is presented by Wosnik and George[21] and for pressure gradient by Castillo[22] and Castillo et al.[23]

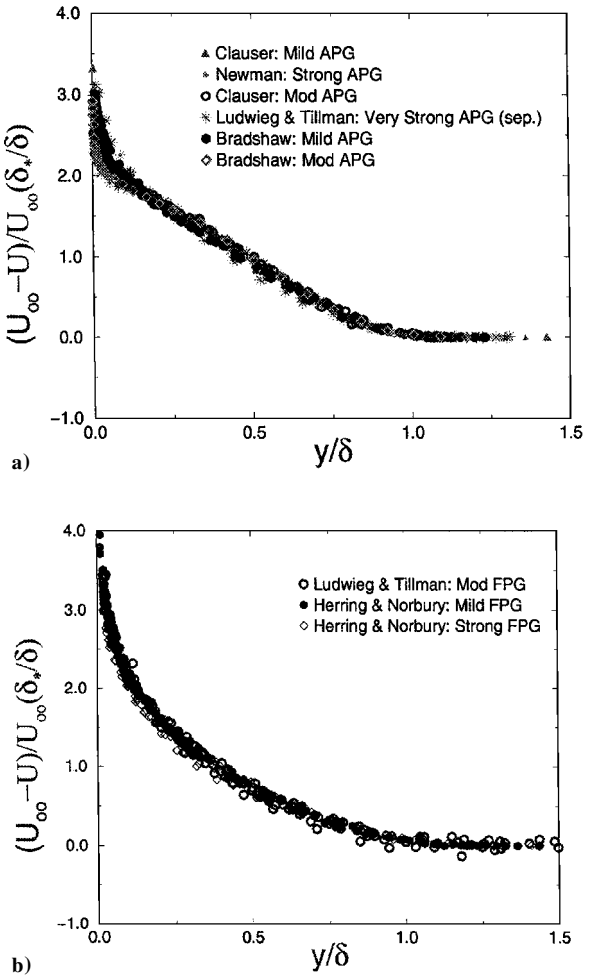

Fig. 8 Velocity profiles normalized by $U_\infty\,\delta_*/\delta_{99}$ data of a) APG and b) FPG.

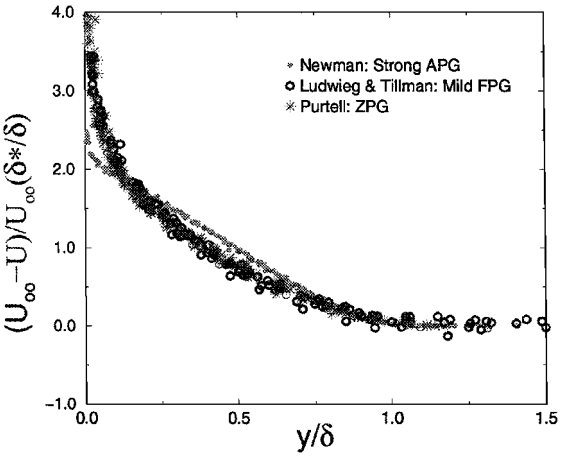

Fig. 9 Combined plot of the three profiles: velocity is normalized by $U_\infty\,\delta_*/\delta$.

That the pressure gradient velocity data yield only two profiles, one for APG and one for FPG, is remarkable but consistent with that there appears to be only two nonzero values of Λ. This follows immediately from Eq. (17). If there are only two nonzero values of Λ, then there can at most be two solutions to the equation. Hence, there can only be two pressure gradient velocity deficit profiles and two corresponding Reynolds stress profiles.

Figure 9 shows both the APG, ZPG, and FPG velocity profiles of Fig. 8 with the similarly normalized ZPG data of Purtell et al.[24] The APG profile is distinctly different from the other two. The differences between the ZPG and FPG profiles are more subtle. As noted earlier, this is consistent with the similarity theory and the apparent fact that there are only three values of Λ: 0.22, 0, and -1.92. Hence, in addition to the two pressure gradient boundary-layerprofiles, there must be a third for the ZPG boundary layer.

Conclusion

It has been shown that most turbulent boundary layers appear to be equilibrium similarity boundary layers where equilibrium boundary layers are defined as $\Lambda = \text{const}$. Contrary to the classical belief that equilibrium flows are special flows and are difficult to achieve in experiments, there appear to be almost no flows that are not in equilibrium, at least by this definition. Interesting, there appear to be only three possible values of Λ: 0.22, 0, and -1.92. The Reynolds averaged equations for the mean motion in similarity variables make it clear then that there can only be three possible limiting velocity profiles in turbulent boundary layers. This appears to be the case, at least when the velocity data are normalized using $U_\infty\, \delta_*/\delta_{99}$.

In summary, the equilibrium similarity analysis has yielded results that are in complete agreement with virtually all of the classical experimental data. Moreover, the success of the theory has raised a number of interesting new avenues for research, both to confirm these ideas and to extend them. One of the most interesting might be to ask how an equilibrium boundary layer can ever separate once it is locked into an equilibrium similarity state. The answer might lead to a whole new understanding of separation, with important ramifications for design.

References

[1]George, W. K., and Castillo, L., "Zero-Pressure Gradient Turbulent Boundary Layer," *Applied Mechanics Reviews*, Pt. 1, Vol. 50, No. 11, 1997, pp. 689–729.

[2]George, W. K., and Castillo, L., "Boundary Layers with Pressure Gradient: Another Look at the Equilibrium Boundary Layer," *Near Wall Turbulent Flows*, edited by R. M. C. So., C. G. Speziale, and B. E. Launder, Elsevier, New York, 1993, pp. 901–910.

[3]Clauser, F. H., "The Turbulent Boundary Layer," *Advances in Applied Mechanics*, Vol. 4, 1954, pp. 1–51.

[4]Clauser, F. H., "The Turbulent Boundary Layer in Adverse Pressure Gradient," *Journal of the Aeronautical Sciences*, Vol. 21, 1954, pp. 91–108.

[5]Bradshaw, P., "The Turbulence Structure of Equilibrium Boundary Layers," NPL Aero. Rept. 1184, 1966.

[6]Ludwieg, H., and Tillmann, W., "Investigations of the Wall Shearing Stress in Turbulent Boundary Layers," NACA TM 1285, 1950.

[7]Townsend, A. A., *The Structure of Turbulent Shear Flows*, 2nd ed., Cambridge Univ. Press, London, 1976.

[8]Townsend, A. A., *The Structure of Turbulent Shear Flows*, Cambridge Univ. Press, Cambridge, England, U.K., 1956.

[9]George, W. K., "Some New Ideas for Similarity of Turbulent Shear Flows," *Turbulence, Heat and Mass Transfer, Lisbon 1994*, edited by K. Hanjalic and J. C. F. Pereira, Begell House, New York, 1995, pp. 24–49.

[10]George, W. K., Castillo, L., and Wosnik, M., "A Theory for Turbulent Pipe and Channel Flows," Theoretical and Applied Mechanics, TAM Rept. 872, UIL-ENG-97-6033, Univ. of Illinois, 1997.

[11]Tennekes, H., and Lumley, J. L., *A First Course in Turbulence*, MIT, Cambridge, MA, 1972.

[12]George, W. K., "Self-Preservation of Turbulent Flows and Its Relation to Initial Conditions and Coherent Structures," *Advances in Turbulence*, edited by W. K. George and R. Arndt, Hemisphere, New York, 1989, pp. 39–73.

[13]Batchelor, G. K., *An Introduction to Fluid Dynamics*, Cambridge Univ. Press, New York, 1966.

[14]Coles, D. E., and Hirst, E. A., *Proceedings: Computation of Turbulent Boundary Layers—1968*, AFOSR–IFP–Stanford Conf., Vol. 2, 1969.

[15]Newman, B. G., "Some Contributions to the Study of the Turbulent Boundary Near Separation," Austr. Dept. Supply Rept. ACA-53, 1951.

[16]Zagarola, M. V., and Smits, A. J., "Mean-Flow Scaling of Turbulent Pipe Flow," *Journal of Fluid Mechanics*, Vol. 373, 1998, pp. 33–79.

[17]Herring, H., and Norbury, J., "Some Experiments on Equilibrium Turbulent Boundary Layers in Favorable Pressure Gradients," *Journal of Fluid Mechanics*, Vol. 27, 1967, pp. 541–549.

[18]Kline, S. J., Reynolds, W. C., Schraub, F. A., and Rundstatler, P. W., "The Structure of Turbulent Boundary Layers," *Journal of Fluid Mechanics*, Vol. 30, No. 4, 1967, pp. 741–773.

[19]Schubauer, G. B., and Klebanoff, P., "Forced Mixing in Boundary Layers," *Journal of Fluid Mechanics*, Vol. 8, No. **XX**, 1950, pp. 10–32.

[20]Castillo, L., "Similarity Analysis of Turbulent Boundary Layers," Ph.D. Dissertation, Dept. of Mechanical and Aerospace Engineering, State Univ. of New York, Buffalo, NY, Feb. 1997.

[21]Wosnik, M., and George, W. K., "Reconciling the Zagarola/Smits Scaling With the George/Castillo Theory For the Zero Pressure Gradient Turbulent Boundary Layer," AIAA Paper 2000-0911, Jan. 2000.

[22]Castillo, L., "Application of Zagarola/Smits Scaling in Turbulent Boundary Layers with Pressure Gradient," *Advances in Fluids Mechanics III*, edited by M. Rahman and C. A. Brebia, 2000, pp. 275–288.

[23]Castillo, L., Walker, D. J., and Wosnik, M., "Implications of the Upstream Conditions on the Downstream Flow in Turbulent Boundary Layers," AIAA Paper 2000-2309, June 2000.

[24]Purtell, L. P., Klebanoff, P. S., and Buckley, F. T., "Turbulent Boundary Layer at Low Reynolds Number," *Physics of Fluids*, Vol. 24, 1981, pp. 802–811.

R. M. C. So
Associate Editor